Title

Mitochondrial DNA deletion mutations increase exponentially with age in human skeletal muscle

Journal

Aging Clinical and Experimental Research, 33(7)

ISSN

1594-0667

Authors

Herbst, Allen
Lee, Cathy C
Vandiver, Amy R
et al.

Publication Date

2021-07-01

DOI

10.1007/s40520-020-01698-7

Peer reviewed

HHS Public Access

Author manuscript

Aging Clin Exp Res. Author manuscript; available in PMC 2022 July 01.

Published in final edited form as:

Aging Clin Exp Res. 2021 July ; 33(7): 1811–1820. doi:10.1007/s40520-020-01698-7.

Mitochondrial DNA deletion mutations increase exponentially with age in human skeletal muscle

Allen Herbst, PhD[1], **Cathy C. Lee, MD**[2,3], **Amy R. Vandiver, MD, PhD**[4], **Judd M. Aiken, PhD**[1], **Debbie McKenzie, PhD**[5], **Austin Hoang, BS**[3], **David Allison, PhD**[6], **Nianjun Liu, PhD**[6], **Jonathan Wanagat, MD, PhD**[*,2,3]

[1]Department of Agricultural, Food and Nutritional Sciences, University of Alberta, Edmonton, Alberta, Canada

[2]Veterans Administration Greater Los Angeles Healthcare System, Los Angeles, USA

[3]Division of Geriatrics, Department of Medicine, UCLA, Los Angeles, California, USA

[4]Division of Dermatology, Department of Medicine, UCLA, Los Angeles, California, USA

[5]Department of Biological Sciences, University of Alberta, Edmonton, Alberta, Canada

[6]Department of Epidemiology and Biostatistics, Indiana University Bloomington, Bloomington, Indiana, USA

Abstract

[*]Correspondence: Jonathan Wanagat, MD, PhD, Division of Geriatrics, Department of Medicine, University of California, Los Angeles, 10945 Le Conte Ave, Suite 2339, Los Angeles, CA 90095, Phone: 310-825-8253, jwanagat@mednet.ucla.edu.

Author Contributions

AH, JMA, DM and JW conceived and planned the experiments. CCL provided the de-identified muscle samples. AH purified DNA and performed all digital PCR measurements. AH, NL, DA, AV and JW analyzed the data. JW and AH wrote the manuscript with input from all authors.

Supplemental Data

One table and one figure are included as supplemental data.

Conflicts of interest/Competing interests

The authors declare no conflicts of interest/competing interests.

Ethics approval (include appropriate approvals or waivers)

Animal studies were conducted according to the Guidelines for Ethical Conduct in the Care and Use of Nonhuman Animals in Research and were approved by the UCLA Institutional Animal Care and Use Committee. De-identified muscle biopsy specimens were collected as part of a VA Merit Award, “Testosterone, inflammation and metabolic risk in older Veterans” and NIH R01DK090406 (PI: Cathy Lee, MD). Use of the human specimens for this study was approved by the UCLA Institutional Review Board (Protocol #18-001547) and the University of Alberta Health Research Ethics Board #00084515.

Consent to participate

This study involved the use of de-identified human muscle biopsies and therefore did not include human subjects.

Consent for publication

This study involved the use of de-identified human muscle biopsies and therefore did not include human subjects.

Availability of data and material

The data that support the findings of this study are available from the corresponding author upon reasonable request.

Background: Mitochondrial DNA (mtDNA) deletion mutations lead to electron transport chain deficient cells and age-induced cell loss in multiple tissues and mammalian species. Accurate quantitation of somatic mtDNA deletion mutations could serve as an index of age-induced cell loss. Quantitation of mtDNA deletion molecules is confounded by their low abundance in tissue homogenates, the diversity of deletion breakpoints, stochastic accumulation in single cells, and mosaic distribution between cells.

Aims: Translate a pre-clinical assay to quantitate mtDNA deletions for use in human DNA samples, with technical and biological validation, and test this assay on human subjects of different ages.

Methods: We developed and validated a high-throughput droplet digital PCR assay that quantitates human mtDNA deletion frequency.

Results: Analysis of human quadriceps muscle samples from 14 male subjects demonstrated that mtDNA deletion frequency increases exponentially with age – on average, a 98-fold increase from age 20-80. Sequence analysis of amplification products confirmed the specificity of the assay for human mtDNA deletion breakpoints. Titration of synthetic mutation mixtures found a lower limit of detection of at least 0.6 parts per million. Using muscle DNA from six-month old mtDNA mutator mice, we measured a 6.4-fold increase in mtDNA deletion frequency (i.e., compared to wild-type mice), biologically validating the approach.

Discussion/Conclusions: The exponential increase in mtDNA deletion frequency is concomitant with the known muscle fiber loss and accelerating mortality that occurs with age. The improved assay permits the accurate and sensitive quantification of deletion mutations from DNA samples and is sufficient to measure changes in mtDNA deletion mutation frequency in healthy individuals across the lifespan and, therefore, patients with suspected mitochondrial diseases.

Keywords

MtDNA; mitochondria; mutation; deletion; sarcopenia; biomarker

Introduction

Age is the primary risk factor for the leading causes of disability and death [1]. While aging has traditionally been classified as a non-modifiable risk factor, this is no longer true. Aging and lifespan are modified routinely in a variety of model organisms, including rodents and nonhuman primates. These age-modifying interventions are now poised for translation to humans, however, experimental read-outs such as survival are not a practical endpoint. Biomarkers are needed to accurately measure the rate of biological aging and predict healthspan and lifespan [2].

Many current biomarkers are neither mechanistic nor sufficiently predictive owing to their lack of proximity to the cellular processes that underlie aging. These markers correlate with chronological age, but do not reflect biological age [3, 4]. MtDNA deletion mutations arise from errors of replication of the mitochondrial genome [5]. These mutation events remove ~4-12 kb of primary mtDNA sequence with the breakpoints for these deletion events typically centered in the mitochondrial major arc [6]. The resulting mutated mtDNA lacks

multiple genes that encode the protein subunits necessary for oxidative phosphorylation (Figure 1A). With time, the deletion clonally accumulates within its individual cell. When the intracellular deletion abundance exceeds 90%, electron transport chain (ETC) function is disrupted and cells lose cytochrome c oxidase (COX) activity prior to undergoing cell death [7]. In 36-month old rat quadriceps, ~80% of the myofibers that are positive for markers of apoptosis and/or necrosis were ETC-deficient. The sequential process of mtDNA deletion formation, clonal accumulation, ETC deficiency, and cell death reiterates in an increasing number of cells with age. MtDNA deletion containing, ETC-deficient cells have been detected in the brain, heart, kidney, and skeletal muscle of aged mammals including humans where they may contribute to the cellular phenotypes and tissue degeneration of aging [8-11].

Cell loss is a significant feature of mammalian aging [12]. MtDNA deletion frequency may serve as a surrogate marker for ETC deficient cells and, thus, the rate of cell loss. In rodents, mtDNA deletion frequency predicts the abundance of ETC deficient cells, as assessed using laborious histochemical staining in skeletal muscle [13]. As these cells ultimately undergo apoptosis and necrosis, steady-state tissue levels of ETC deficient cells remain low. The instantaneous mtDNA deletion frequency could approximate the *in vivo* rate of age-induced cell loss.

A critical barrier to understanding the contribution of mtDNA deletions to aging has been the requirement for both sensitive and specific methods of quantitation. The magnitude of deletion mutation abundance in tissue homogenates distinguishes aging from genetic diseases such as the mitochondrial myopathies. In rat muscle, mtDNA deletion mutations increase ~60 fold between 12- and 34-months of age and the absolute magnitude in tissue homogenates rises to 0.12% [13]. High specificity is also required as wild type mtDNA, which (in homogenates) is in excess, contains the same PCR priming sites as those present in mtDNA deletion molecules. Moreover, as most mtDNA deletion mutations contain unique breakpoints, the assay needs to detect a heterogeneous class of molecules [6]. A "common" mtDNA deletion mutation "4,977" has been identified to increase in abundance with age [14] and is associated with some inherited mitochondrial myopathies [15], however, this mutation has only rarely been detected in ETC deficient muscle fibers from aged humans [6, 16]. Rather, numerous unique mtDNA deletion mutations accumulate to high levels in ETC deficient human cells [6].

We have overcome the barrier to accurate quantitation of mtDNA deletion frequency with a novel digital PCR (dPCR) assay that brings numerous advantages [13]. We adapted a direct digital PCR method originally developed in rodent models [13, 17]. First, this approach is capable of detecting a diverse population of mtDNA deletions across the major arc, rather than focusing on a single deletion species such as the “common” deletion [18-20]. Second, digital PCR permits absolute mutation quantitation without the need for standard curves as required for real-time PCR. Digital PCR assays utilize end-point analysis of each partition to generate quantitative data and are independent of PCR efficiency. This independence from PCR efficiency permits the equivalent detection of deletions despite amplicon size differences. Finally, the new assay directly measures deletion mutation abundance, which is more accurate than indirect approaches that infer deletion mutation frequency by absence of

major arc site amplification [13]. The lower limit of detection (LLOD) for deletion mutation frequency using the indirect approach has been validated to be 2.5% [21], and 25% [13]. In rats, a direct approach to quantifying deletion mutations using chip-based dPCR had a LLOD of 0.03% [18].

Here we adapted and refined the direct digital PCR approach to quantify human mtDNA deletion mutations from vastus lateralis muscle biopsy samples across the lifespan. The adapted assay benefits from a droplet dPCR format that increases throughput and thus replicate number, decreases cost, and automates sample preparation. Initial validation of the direct deletion droplet digital PCR (4DPCR) assay was performed, confirming the assay specificity, and sensitivity. We show that mtDNA deletion mutation frequency increases exponentially with age in human skeletal muscle.

Materials and Methods

Ethics statement

Animal studies were conducted according to the Guidelines for Ethical Conduct in the Care and Use of Nonhuman Animals in Research and were approved by the UCLA Institutional Animal Care and Use Committee. De-identified muscle biopsy specimens were collected as part of a VA Merit Award, “Testosterone, inflammation and metabolic risk in older Veterans” and NIH R01DK090406 (PI: Cathy Lee, MD). Use of the human specimens for this study was approved by the UCLA Institutional Review Board (Protocol #18-001547) and the University of Alberta Health Research Ethics Board #00084515.

Tissue samples

De-identified human muscle biopsy samples were obtained from the quadriceps muscle of 14 male subjects ranging in age from 20 to 81 years [22]. Mouse quadriceps muscle samples were obtained from 6-month-old wild-type, heterozygous, and homozygous mutator mice (Stock No:017341, PolgA^{D257A}) purchased from The Jackson Laboratory (Bar Harbor, ME). Anonymous-donor, non-irradiated platelet concentrate from a 69yo woman was purchased from a commercial biobank (Amsbio, Abingdon, United Kingdom). Platelet concentrates were pelleted as previously described [23]. All samples were flash-frozen in liquid nitrogen and stored at −80 Celsius until DNA isolation. Personnel analyzing human muscle biopsy samples were blinded to subject age. Subject ages were only revealed after analyses were completed.

DNA isolation and quality control

Tissue samples were powdered under liquid nitrogen using a mortar and pestle. Approximately 25mg of powdered muscle was used for DNA isolation, performed by proteinase K and RNase A digestion, phenol/chloroform extraction, and ethanol precipitation, as previously described [13]. Quality control of the DNA was performed via Nanodrop (Nanodrop 2000, Thermo Scientific; Waltham, MA), Qubit (2.0, Invitrogen; Carlsbad, CA), and Tapestation (2200, Agilent; Santa Clara, CA). Platelet total DNA samples were determined to be >99% mtDNA (data not shown).

Droplet digital PCR

A 5’ nuclease cleavage assay and droplet digital PCR (ddPCR) were used to quantitate copy numbers for nuclear DNA, total mtDNA, and mtDNA deletions with specific primer/probe sets and cycling conditions for each (Supplemental Table 1). Samples were diluted to the manufacturer’s recommended target range (1 to 5,000 copies per microliter) in 25 microliter reactions using BioRad ddPCR Supermix for Probes (BioRad; Hercules, CA). Final primer and probe concentrations were 900nM and 250nM, respectively. Reactions were partitioned into droplets using a BioRad QX200 Droplet Generator (BioRad; Hercules, CA) prior to thermocycling. Digital PCR cycling conditions for nDNA and mtDNA copy number included Taq-polymerase activation at 95°C for ten minutes, followed by 40 cycles of denaturation at 94°C for 30 seconds and annealing/extension at 60°C for two minutes. Droplet fluorescence was then read using a BioRad QX200 Droplet Reader. Target copy numbers per microliter were determined using BioRad QuantaSoft Regulatory Edition Software (Version 1.7, BioRad; Hercules, CA). Direct quantitation of major arc deletions by ddPCR used cycling conditions of Taq-polymerase activation at 95°C for ten minutes, followed by 60 cycles of: denaturation at 94°C for 15 seconds, annealing at 55°C for one minute, and extension at 72°C for six minutes. Deletion assays on mouse skeletal muscle DNA used mouse-specific primer/probe sets shown in Supplementary Table 1 [13], with the same cycling conditions as described for the human mtDNA major arc deletion detection.

Droplet PCR amplicon isolation and sequencing

Droplet digital PCR reactions were pooled to provide sufficient starting material. Pooled reactions were extracted with chloroform according to manufacturer’s protocols to isolate DNA for sequencing (Bio-Rad Laboratories, Hercules, CA).

Next generation sequencing (NGS) was performed using a commercially available system (Illumina, San Diego, CA). Purified droplet amplicons were fragmented using a focused-ultrasonicator (M220, Covaris, Woburn, MA) prior to library preparation. DNA libraries were constructed using the KAPA HyperPlus Kit (Roche, Basel, CH). Sequencing was performed on the Illumina MiSeq desktop sequencer using the 600-cycle MiSeq Reagent V3 Kit (Illumina, San Diego, CA). Sequence data was aligned to the revised Cambridge Sequence (rCS, NC_012920.1) using BWA v0.7.17. Data complexity was reduced to a random sample of 1 million (of ~37 million) reads aligned to the target region (bp 5707 to 16529). These data were input into eKLIPse software (v1.8 [24]), an algorithm for mtDNA deletion finding based on soft-clipping. Default parameters (including a minimum deletion size of 1Kb) were used.

Synthetic human deletion mutations and mixing experiments

Double-stranded DNA targets representing deletion mutation targets were synthetically generated (ATUM, Newark, CA) in a PUC57 vector. Quality control of the DNA was performed as described above. Synthetic human deletion target was mixed with serial 10-fold dilutions of wild-type mtDNA isolated from human platelets. The background mutation frequency of human platelet sample was 2.1e-7. The synthetic human deletion target was kept at a constant copy number while wild type mtDNA molecules were added at increasing concentrations.

Statistical analysis

All data are presented as mean ± SEM. In analyses of mutator mouse samples, ANOVA was used to compare differences among multiple groups, followed by Tukey's multiple comparison test for significance between the different genotypes. Statistical analyses including regression analyses were performed using GraphPad Prism (version 7.05, GraphPad).

Results

Design of human mtDNA direct deletion droplet digital PCR (4DPCR) assay

To quantitate age-induced human mtDNA deletions, we adapted our chip-based digital PCR approach [13] to droplet dPCR. As in the earlier chip-based method, quantitation of mtDNA deletion mutations relies on the selective amplification of the smaller genomes (resulting from the loss of a significant portion of the mitochondrial major arc). With forward and reverse PCR primers flanking the major arc, the deletion mutations permit PCR amplification under a constrained PCR extension time that would otherwise not occur on wild-type molecules (Figure 1A) [13, 25-28]. A primer set to quantify total mtDNA (i.e., wild-type mtDNA and mtDNA deletions) is positioned in the minor arc (12S rRNA gene), a region of the mtDNA that is preserved with age [6]. Nuclear DNA copy number is quantitated by assay of RNase P, a single copy nuclear gene. Minor arc deletions, deletions that remove primer/probe sites, or very small mtDNA deletion events (i.e. events that remove only a few hundred basepairs) would not be detected by the assay.

Digital PCR partitions individual mtDNA templates into droplets. Following thermocycling, droplets are either positive or negative depending on PCR amplification and the level of fluorescent probe hydrolysis (Figure 1B). The fluorescent signal in positive droplets is indicative of the level of probe hydrolysis and thus PCR efficiency of an individual amplification product. Differing droplet patterns in the 1D fluorescence amplitude plot are observed between individuals while technical replicates show similar amplitude patterns.

Assay Validation

Following droplet digital PCR, we recovered the amplification products from the droplets and verified their mtDNA origins (Figure 2). Deletion mutation breakpoints were identified by next-generation sequencing analysis of droplet digital amplification products (Figure 2D, E). To further characterize the size range of deletions detected by the assay, we used restriction digestion of a quadriceps muscle DNA sample from an 86yo woman to restrict the population of amplifiable deletion molecules to those mtDNA molecules with deletions greater than 8kb, 6Kb, 4Kb and 2Kb (Supplementary Fig. 1). These data demonstrate that there is an amplification limit that corresponds to: 1) the extension time allowed in the reaction (i.e., 6 minutes), 2) the distribution of mtDNA deletion breakpoints identified from ETC deficient fibers [6] and 3) those deletions detected by next generation sequencing analysis (Figure 2C, D, E).

We next examined the lower limit of detection (LLOD) of the assay by quantitating defined mixtures of a synthetic human deletion mutation with highly enriched wild-type human

mtDNA. In these spike-in experiments, the lower level of detection was below 0.6 parts per million. The quantification was linear across seven orders of magnitude (R^2 =.9969, Figure 3A). Amplification and detection of deletions was unaffected by the addition of increasing amounts of highly enriched wild-type mitochondrial DNA (Figure 3A) isolated from human platelets. A deletion frequency of 0.6 ppm is >20-fold lower than what we have observed in human and rodent muscle samples.

This sensitivity was sufficient to quantitate the abundance of mtDNA deletions in muscle homogenates from control and mtDNA mutator mice used as positive controls (Figure 3B). In the mutator mouse muscle, we quantitated mutation frequencies ranging from 0.0006% in 6mo WT mice, 0.0005% in 6mo heterozygous mutator mice and 0.0032% in homozygous 6mo mutator mice. In this genetic mouse model, deletion mutation frequency was not different (p=.8935) between wild-type and heterozygous mice, but on average was 640% higher in the shorter-lived, homozygous mutator mice (p<.0001). This 6.4-fold increase of deletion frequency in mutator mouse muscle is similar to the seven to eleven fold increase reported in homozygous mutator mouse brain and heart as compared to WT and heterozygous mutator mice [29].

Decrease in human muscle mtDNA copy number with age.

To calculate mtDNA deletion frequency, it is necessary to first measure total mtDNA copy number per diploid nucleus. We found a significant, non-zero negative correlation between total vastus lateralis mtDNA copy number per diploid nucleus and age (Figure 4) ([mtDNA copy no. / diploid nucleus] = −58.22*Age+7046, r=−0.782, p=0.0009). On average mtDNA copy number decreased by 2.5-fold between ages 20 and 80.

Exponential increase in human muscle mtDNA deletion frequency

We measured deletion mutation frequency in vastus lateralis muscle biopsy samples from subjects between ages 20 to 81. MtDNA deletion mutation frequency ranged from $2.60x10^{-6}$ in an individual at age 20 to $2.04x10^{-3}$ in an individual at 81-years of age (Figure 5A). The increase was exponential and log transformation linearized the relationship between deletion frequency and age (Log[Deletion Frequency] = 0.03321*Age-5.827, r=0.747, p=0.0021) (Figure 5B). From the regression line, on average, deletion frequency increased 98-fold with age.

Discussion

MtDNA deletion mutations reflect a specific cellular event tied to aging. MtDNA deletion mutations do not accumulate silently; their intracellular accumulation induces phenotypic changes leading to cell dysfunction and death, and cell loss, which negatively affects tissue structure and function [7, 8, 10, 11, 30-33]. Previously, we demonstrated that mtDNA deletion frequency strongly predicts the abundance of electron transport chain deficient cells as assessed histochemically [13]. The correlation coefficient between deletion frequency and ETC deficient fiber number measured from the same samples was found to be 0.99. The tight correlation of mtDNA deletion frequency by 4DPCR and ETC deficient fiber number allows us to use this assay as a surrogate marker of these underlying cellular events. As ETC

deficient cells induce apoptosis, necrosis and lead to cell loss [7], we reasoned that mtDNA deletion frequency may serve as a predictor of cell loss.

To place the exponential increase in vastus lateralis deletion frequency in the context of other known measures of human aging, we compared (Figure 5C) vastus lateralis muscle fiber number from Lexell *et al.* [34] with human male survival data from the Social Security Administration period 2015 life table [35]. The exponential phase of increasing deletion frequency is concomitant with the loss of muscle fibers that accelerates at approximately age 60 and the accelerating mortality that defines human aging. The change in magnitude of fiber loss is not equivalent to the change in magnitude of deletion mutation frequency. The fiber number (loss) is indicative of the cumulative impact of deletion mutations, whereas the mutation frequency is the instantaneous burden of deletions. A caveat to the plot in Figure 5C is that the deletion frequency data was not generated from the same samples as the fiber loss data. It is unlikely that total fiber number will be reexamined in whole human vastus lateralis samples. Additional comparisons should be examined between deletion mutation frequency and performance measures in the same subjects such as VO2Max, 6-minute walk, or grip strength.

Because chronological age and biological age are not directly correlated, a biomarker predictive of an individual's rate of biological aging will likely not accurately reflect chronological age and vice versa. The relationship between available biomarkers, such as mtDNA copy number shown in Figure 4, and chronological age is often described as linear [36]. It is well understood that mortality increases exponentially as chronological age advances linearly [37]. Processes that contribute to aging and mechanism-proximal biomarkers must also increase exponentially in similar timeframes as mortality if they are to be predictive. In this context, mtDNA deletion frequency may bridge a gap between linear biomarkers of aging and the exponentially accelerating wall of morbidity and mortality that sets health- and lifespans [4]. We observed a correlation coefficient of 0.739 between chronological age and deletion frequency. This level of correlation arises from the diverse outcomes possible for individuals of the same chronological age who have differing biological ages. For example, our dataset contains two 81-year old individuals with a 20-fold range of deletion mutation frequencies. We interpret this finding to reflect that amongst the population of 81-year-olds there are those of differing functional ability with increasingly variable outcomes. Some octogenarians are homebound and have meals delivered, while other 80-year old individuals may be the ones delivering those meals. The predictive accuracy of chronological age and sex for 5-year survival is 0.69 across a large number of studies [38]. A predictive biomarker of human aging must encompass this diversity of biological aging. The observed level of correlation between deletion frequency and chronological age likely reflects the stochastic nature of human aging.

Bulk measurement of mtDNA deletion frequency or ETC deficient cell abundance have been criticized as being too low to have any relevance for aging [39]. Such critiques suggest that magnitude is a prerequisite for causality and ignore the well-established, detrimental cellular impact of these mutations. Deletion mutations clonally expand focally in individual cells to cause cell death [7]. The cumulative loss of cells in muscles and other tissues irreversibly contributes to the aged phenotype. The importance of deletion mutations even at “low”

magnitudes is illustrated by comparison with the human fiber number data. Vastus lateralis fiber number declines from ~600,000 at 50 years of age to ~323,000 at 80 years; on average ~25 fibers (~0.008%) are lost every day [40]. Thus, while the deletion frequency and ETC deficient cell abundance are "low," so too is the insidious and progressive cell loss and muscle dysfunction. The magnitudes of deletion frequency, ETC deficient cell abundance and the rate of fiber loss distinguish aging from disease. When examining biomarkers in a cross-sectional study, the data one collects are indicative of steady state levels. These levels do not encompass the whole of the phenomena that compound across a lifespan. The steady state levels must be of lower magnitude.

While the spectrum of breakpoints we sequenced from the digital PCR droplets is typical of deletions found by single cell PCR and breakpoint sequencing [6, 8, 41, 42], the breakpoints amplified are not necessarily representative of the entire spectrum of mtDNA deletion mutations that exist *in vivo*. For example, we did not observe the 4,977 deletion breakpoint in the next generation sequencing data, even though this deletion is known to increase with age in muscle [27]. The distribution of droplet amplitudes (Figure 1B) is due to the differing sizes of the underlying deletion mutations [18]. Larger mtDNA deletion mutations give rise to smaller amplification products resulting in higher endpoint fluorescence amplitude. The variable distribution of fluorescent signals observed in the positive droplets indicates the presence of multiple deletion species as would be expected from aged individuals.

Our deletion frequency measurements are not derived from amplification of nuclear mtDNA sequences (Numts) [43]. Digital PCR quantitation is dependent on having a substantial number of partitions that do not amplify. For an LLOD of 0.6 ppm, it is necessary to add DNA in excess to the reaction mixture. The consequence is that each droplet has numerous copies of wild-type mitochondrial DNAs as well as nuclear DNA that could be amplified if the reaction is not specific. In properly prepared reactions, a large fraction of droplets should not demonstrate amplification. Secondly, the distance between the primers is such that the amplification of Numts is improbable for the same reason that this assay does not amplify wild-type mtDNA. Finally, NCBI Primer-BLAST analysis for off-target amplification does not demonstrate any amplicons in the *Homo sapiens* nuclear genome that would be detectable with our 4DPCR primer/probe set.

The lack of accurate measurement of mtDNA deletion frequency has confounded the clinical assessment of primary and secondary mitochondrial diseases [44]. Molecular measurement of mtDNA deletion frequency will allow clinicians to monitor disease progression and assist with the development and testing of disease-modifying therapies [45, 46]. Accurate quantitation of deletion mutation frequency would also aid the identification of environmental exposures or weak genetic polymorphic effectors that affect mtDNA quality and how mtDNA quality changes with age. The 4DPCR assay addresses these challenges by providing a high-throughput method amenable to any DNA sample for measurement of mtDNA deletions to an LLOD of at least 0.6 ppm.

Further validation of the assay, in accordance with published guidelines for clinical bioanalytical assays [47], would provide the requisite rigor and reproducibility for use of mtDNA deletion frequency in longitudinal studies of aging. Such studies may enable the use

of mtDNA deletion frequency as a predictor of human biological age; independent of chronological age and sex. Adaptation of this assay to other clinical samples including peripheral blood would enable broader application of the assay in clinical trials of human aging interventions, especially those targeting metabolism and mitochondrial biology.

Supplementary Material

Refer to Web version on PubMed Central for supplementary material.

Acknowledgments

Funding

This work is supported by the National Institute on Aging at the National Institutes of Health (grant numbers R56AG060880, R01AG055518, K02AG059847, and R21AR072950).

References

1. Kaeberlein M, Longevity and aging. F1000Prime Rep, 2013. 5: p. 5. [PubMed: 23513177]
2. Ferrucci L, et al., Measuring biological aging in humans: A quest. Aging Cell, 2020. 19(2): p. e13080. [PubMed: 31833194]
3. Miller RA, Biomarkers of Aging. http://www-personal.umich.edu/~millerr/Biomarkers.htm, 2001.
4. Finch CE and Crimmins EM, Constant molecular aging rates vs. the exponential acceleration of mortality. Proc Natl Acad Sci U S A, 2016. 113(5): p. 1121–3. [PubMed: 26792520]
5. Oliveira MT, Pontes CB, and Ciesielski GL, Roles of the mitochondrial replisome in mitochondrial DNA deletion formation. Genet Mol Biol, 2020. 43(1 suppl. 1): p. e20190069. [PubMed: 32141473]
6. Bua E, et al., Mitochondrial DNA-deletion mutations accumulate intracellularly to detrimental levels in aged human skeletal muscle fibers. Am J Hum Genet, 2006. 79(3): p. 469–80. [PubMed: 16909385]
7. Cheema N, et al., Apoptosis and necrosis mediate skeletal muscle fiber loss in age-induced mitochondrial enzymatic abnormalities. Aging Cell, 2015. 14(6): p. 1085–93. [PubMed: 26365892]
8. Wanagat J, et al., Mitochondrial DNA deletion mutations colocalize with segmental electron transport system abnormalities, muscle fiber atrophy, fiber splitting, and oxidative damage in sarcopenia. FASEB J, 2001. 15(2): p. 322–32. [PubMed: 11156948]
9. Ekstrand MI, et al., Progressive parkinsonism in mice with respiratory-chain-deficient dopamine neurons. Proc Natl Acad Sci U S A, 2007. 104(4): p. 1325–30. [PubMed: 17227870]
10. McKiernan SH, et al., Adult-onset calorie restriction delays the accumulation of mitochondrial enzyme abnormalities in aging rat kidney tubular epithelial cells. Am J Physiol Renal Physiol, 2007. 292(6): p. F1751–60. [PubMed: 17344189]
11. Baris OR, et al., Mosaic Deficiency in Mitochondrial Oxidative Metabolism Promotes Cardiac Arrhythmia during Aging. Cell Metab, 2015. 21(5): p. 667–77. [PubMed: 25955204]
12. Warner HR, Hodes RJ, and Pocinki K, What does cell death have to do with aging? J Am Geriatr Soc, 1997. 45(9): p. 1140–6. [PubMed: 9288026]
13. Herbst A, et al., Digital PCR Quantitation of Muscle Mitochondrial DNA: Age, Fiber Type, and Mutation-Induced Changes. J Gerontol A Biol Sci Med Sci, 2017. 72(10): p. 1327–1333. [PubMed: 28460005]
14. Corral-Debrinski M, et al., Mitochondrial DNA deletions in human brain: regional variability and increase with advanced age. Nat Genet, 1992. 2(4): p. 324–9. [PubMed: 1303288]
15. Wallace DC, Diseases of the mitochondrial DNA. Annu Rev Biochem, 1992. 61: p. 1175–212. [PubMed: 1497308]
16. Yu-Wai-Man P, et al., Somatic mitochondrial DNA deletions accumulate to high levels in aging human extraocular muscles. Invest Ophthalmol Vis Sci, 2010. 51(7): p. 3347–53. [PubMed: 20164450]

17. Herbst A, et al., Mitochondrial DNA alterations in aged macrophage migration inhibitory factor-knockout mice. Mech Ageing Dev, 2019. 182: p. 111126. [PubMed: 31381889]
18. Taylor SD, et al., Targeted enrichment and high-resolution digital profiling of mitochondrial DNA deletions in human brain. Aging Cell, 2014. 13(1): p. 29–38. [PubMed: 23911137]
19. Bielas J, et al., Long term rapamycin treatment improves mitochondrial DNA quality in aging mice. Exp Gerontol, 2018. 106: p. 125–131. [PubMed: 29486228]
20. O'Hara R, et al., Quantitative mitochondrial DNA copy number determination using droplet digital PCR with single-cell resolution. Genome Res, 2019. 29(11): p. 1878–1888. [PubMed: 31548359]
21. Belmonte FR, et al., Digital PCR methods improve detection sensitivity and measurement precision of low abundance mtDNA deletions. Sci Rep, 2016. 6: p. 25186. [PubMed: 27122135]
22. Lee CC, et al., Enhanced Methods for Needle Biopsy and Cryopreservation of Skeletal Muscle in Older Adults. J Cytol Histol, 2020. 11(2).
23. Slichter SJ and Harker LA, Preparation and storage of platelet concentrates. Transfusion, 1976. 16(1): p. 8–12. [PubMed: 3000]
24. Goudenege D, et al., eKLIPse: a sensitive tool for the detection and quantification of mitochondrial DNA deletions from next-generation sequencing data. Genet Med, 2019. 21(6): p. 1407–1416. [PubMed: 30393377]
25. Cao Z, et al., Mitochondrial DNA deletion mutations are concomitant with ragged red regions of individual, aged muscle fibers: analysis by laser-capture microdissection. Nucleic Acids Res, 2001. 29(21): p. 4502–8. [PubMed: 11691938]
26. Shoffner JM, et al., Spontaneous Kearns-Sayre/chronic external ophthalmoplegia plus syndrome associated with a mitochondrial DNA deletion: a slip-replication model and metabolic therapy. Proc Natl Acad Sci U S A, 1989. 86(20): p. 7952–6. [PubMed: 2554297]
27. Cortopassi GA and Arnheim N, Detection of a specific mitochondrial DNA deletion in tissues of older humans. Nucleic Acids Res, 1990. 18(23): p. 6927–33. [PubMed: 2263455]
28. Lee CM, et al., Multiple mitochondrial DNA deletions associated with age in skeletal muscle of rhesus monkeys. J Gerontol, 1993. 48(6): p. B201–5. [PubMed: 8227987]
29. Vermulst M, et al., DNA deletions and clonal mutations drive premature aging in mitochondrial mutator mice. Nat Genet, 2008. 40(4): p. 392–4. [PubMed: 18311139]
30. Bua EA, et al., Mitochondrial abnormalities are more frequent in muscles undergoing sarcopenia. J Appl Physiol (1985), 2002. 92(6): p. 2617–24. [PubMed: 12015381]
31. Wanagat J, Wolff MR, and Aiken JM, Age-associated changes in function, structure and mitochondrial genetic and enzymatic abnormalities in the Fischer 344 x Brown Norway F(1) hybrid rat heart. J Mol Cell Cardiol, 2002. 34(1): p. 17–28. [PubMed: 11812161]
32. Pak JW, et al., Mitochondrial DNA mutations as a fundamental mechanism in physiological declines associated with aging. Aging Cell, 2003. 2(1): p. 1–7. [PubMed: 12882328]
33. Someya S, et al., The role of mtDNA mutations in the pathogenesis of age-related hearing loss in mice carrying a mutator DNA polymerase gamma. Neurobiol Aging, 2008. 29(7): p. 1080–92. [PubMed: 17363114]
34. Lexell J, Taylor CC, and Sjostrom M, What is the cause of the ageing atrophy? Total number, size and proportion of different fiber types studied in whole vastus lateralis muscle from 15- to 83-year-old men. J Neurol Sci, 1988. 84(2-3): p. 275–94. [PubMed: 3379447]
35. Administration, S.S. Actuarial Life Table. 2015; Available from: https://www.ssa.gov/oact/STATS/table4c6.html.
36. Belsky DW, et al., Eleven Telomere, Epigenetic Clock, and Biomarker-Composite Quantifications of Biological Aging: Do They Measure the Same Thing? Am J Epidemiol, 2018. 187(6): p. 1220–1230. [PubMed: 29149257]
37. Gompertz B, On the nature of the function expressive of the law of human mortality and on a new model of determining life contingencies. Phil. Trans. R. Soc, 1825. 115: p. 513–585.
38. Studenski S, et al., Gait speed and survival in older adults. JAMA, 2011. 305(1): p. 50–8. [PubMed: 21205966]
39. Hepple RT, Mitochondrial involvement and impact in aging skeletal muscle. Front Aging Neurosci, 2014. 6: p. 211. [PubMed: 25309422]

40. Lexell J, Downham D, and Sjostrom M, Distribution of different fibre types in human skeletal muscles. Fibre type arrangement in m. vastus lateralis from three groups of healthy men between 15 and 83 years. J Neurol Sci, 1986. 72(2-3): p. 211–22. [PubMed: 3711935]

41. Herbst A, et al., Accumulation of mitochondrial DNA deletion mutations in aged muscle fibers: evidence for a causal role in muscle fiber loss. J Gerontol A Biol Sci Med Sci, 2007. 62(3): p. 235–45. [PubMed: 17389720]

42. Gokey NG, et al., Molecular analyses of mtDNA deletion mutations in microdissected skeletal muscle fibers from aged rhesus monkeys. Aging Cell, 2004. 3(5): p. 319–26. [PubMed: 15379855]

43. Hazkani-Covo E, Zeller RM, and Martin W, Molecular poltergeists: mitochondrial DNA copies (numts) in sequenced nuclear genomes. PLoS Genet, 2010. 6(2): p. e1000834. [PubMed: 20168995]

44. Parikh S, et al., Diagnosis of 'possible' mitochondrial disease: an existential crisis. J Med Genet, 2019. 56(3): p. 123–130. [PubMed: 30683676]

45. Rahman S, Mitochondrial disease in children. J Intern Med, 2020.

46. Ahmed ST, et al., Diagnosis and Treatment of Mitochondrial Myopathies. Neurotherapeutics, 2018. 15(4): p. 943–953. [PubMed: 30406383]

47. Bioanalytical Method Validation Guidance for Industry, U.S. Department of Health and Human Services, Food and Drug Administration, and Center for Drug Evaluation and Research, Editors. 2018.

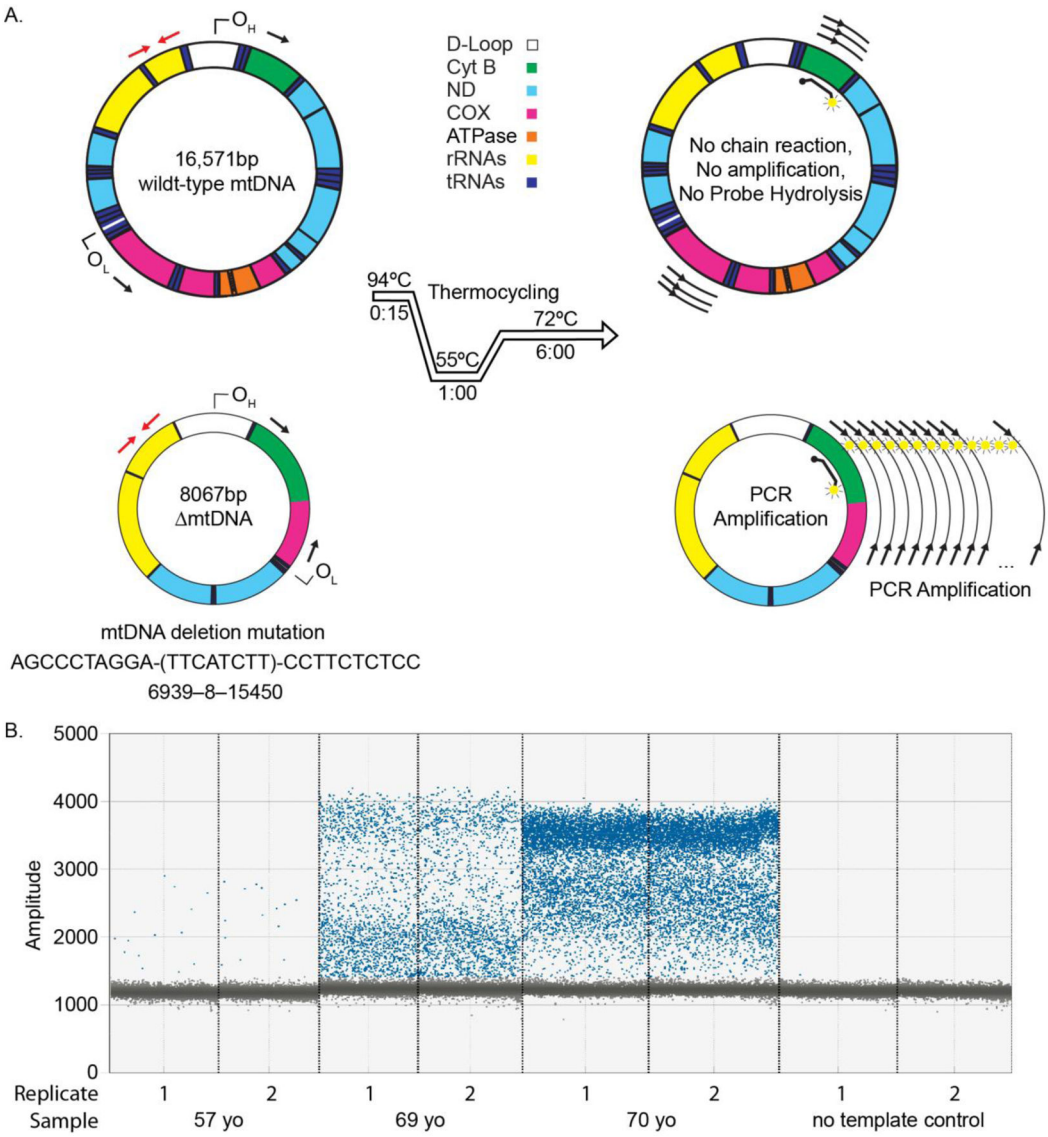

Figure 1. Direct deletion droplet digital PCR assay for measuring human mtDNA deletion mutation frequency.

A. PCR primers are positioned on the human mitochondrial genome to amplify a control region in rRNA (red arrows) for quantifying total mtDNA. A second set of PCR primers flanks the mitochondrial major arc and spans a distance of 10,841 base pairs (black arrows) in wild-type molecules. In wild-type molecules, this region is not amplified when extension time is limited (A, upper row). In mtDNA molecules bearing a representative deletion mutation, this region is amplified (A, lower row). Probe hydrolysis gives rise to the signal. The probe is only hydrolyzed when the 5' primer (near OL) completely extends across the major arc. B. 1D fluorescence amplitude plot from four different vastus lateralis DNA samples in replicate. Blue points are droplets whose fluorescence signal amplitude is above the threshold value ('positives'), while gray points are those droplets whose amplitudes are below the threshold value ('negatives').

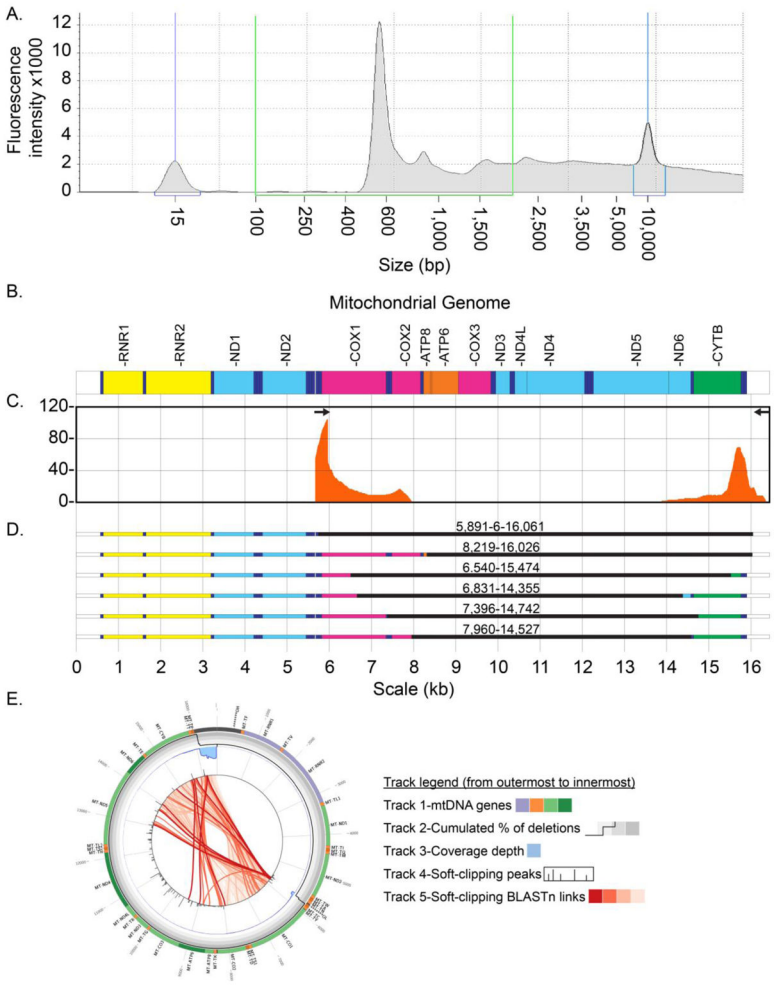

Figure 2. Characterization of amplicons recovered from the 4DPCR assay.

A. Electropherogram of amplicons extracted from droplets following digital PCR amplification. B. Linear representation of the wild-type mitochondrial genome. C. Sequencing read coverage of amplicons extracted from droplets following digital PCR amplification. Sequencing coverage is mapped to the human mtDNA sequence with number of reads (x1,000) shown on the ordinate. The black arrows indicate the PCR primer sites. D. MtDNA deletion mutations identified by next generation sequencing of the PCR reaction droplets. The region in black indicates the portion of the mitochondrial genome missing in the deletion mutation. E. Mapping of mtDNA deletion breakpoints from 4D PCR. The outer Track 1 illustrates the human mitochondrial genome with annotated transfer RNAs (tRNAs) (orange), ribosomal RNAs (rRNAs) (purple), protein-coding genes (green), and noncoding regions (black). The four levels of grey in Track 2 depict the cumulative percentage of deletions, which are denoted by the black line for each mtDNA position. The coverage depth at each base is shown as a blue area, whereas the median coverage of all samples is represented as the dark blue line in Track 3. Soft-clipping peaks are shown in Track 4 as black bars. The size of each bar is proportional to the number of soft-clipped sequences. Bidirectional BLASTs representing deletions are denoted by red arcs with intensities (from

light red to dark red) proportional to the abundance of each amplified deletion event. The plot was produced using eKLIPse software, v1.8 [24].

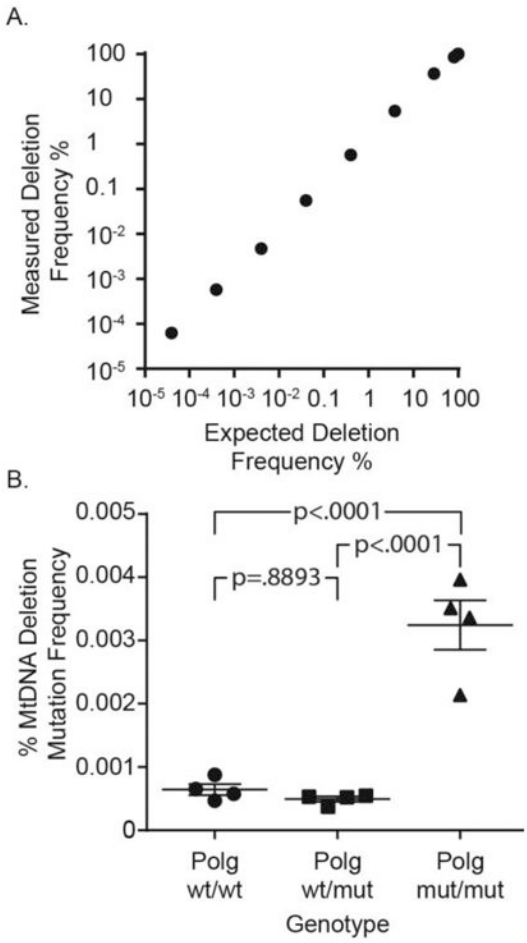

Figure 3. Limit of detection and biological validation of the deletion assay.

A. Percent human mtDNA deletion mutations measured in a spike-in experiment using a synthetic mutation target and purified human mtDNA. Mutation frequency was measured over eight orders of magnitude of known mutation frequency. B. Using mouse mtDNA specific primers in the assay, mtDNA deletion mutation frequency was measured in 6-month-old wild-type ($Polg^{wt/wt}$), heterozygous ($Polg^{wt/mut}$), and homozygous ($Polg^{mut/mut}$) polymerase gamma mutator mice. Bars denote mean ± SEM.

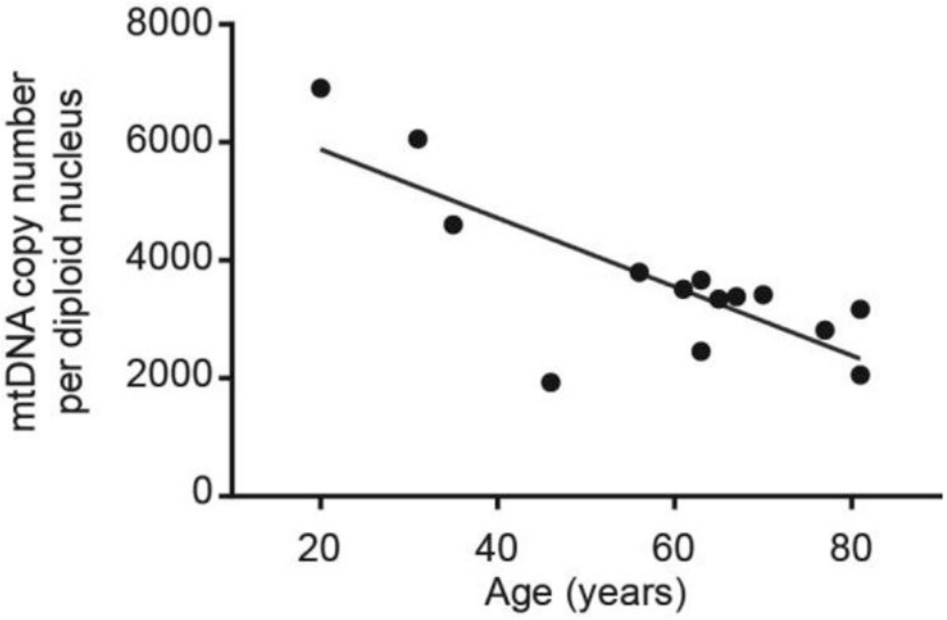

Figure 4. MtDNA copy number declines with age.

MtDNA copy number was measured from human vastus lateralis muscle biopsy samples across the lifespan (r=−0.782). MtDNA copy number was normalized to diploid nuclear DNA copy number as measured by digital PCR quantitation of the single copy gene - RNase P.

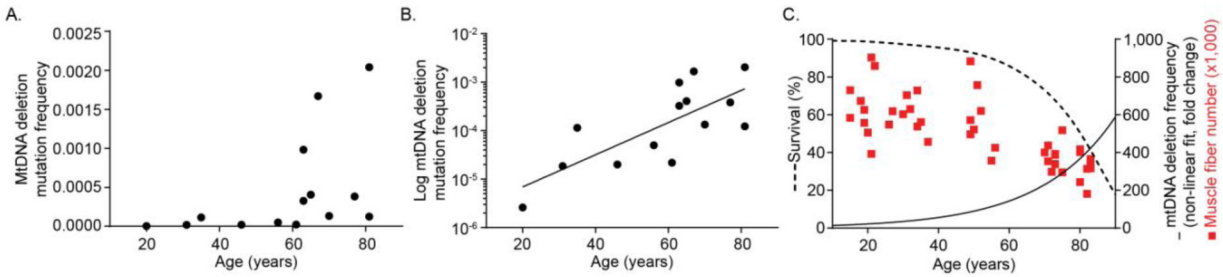

Figure 5. MtDNA deletion mutation frequency increases exponentially with age and parallels previously determined vastus lateralis fiber number and human survival.

A. mtDNA deletion mutations measured from human vastus lateralis muscle biopsy samples across the lifespan. At ages above 60, deletion mutation frequency rises from the baseline. B. Logarithmic transformation of the Y-axis shows the exponential increase (>100 fold) in deletion mutation frequency with age (r=0.747). C. Human survival [35] (dotted line, left axis), vastus lateralis muscle fiber number [34] (red squares, right axis) and non-linear fit of vastus lateralis mtDNA deletion mutation frequency as the fold-change versus a 20-year old subject (black line, right axis) were plotted on the same axis.